Chapter 6

TCP-Fluorapatite Composite Scaffolds: Mechanical Characterization and *In Vitro*/*In Vivo* Testing

Achouak Elghazel, Rym Taktak, Jamel Bouaziz, Slim Charfi and Hassib Keskes

Additional information is available at the end of the chapter

http://dx.doi.org/10.5772/intechopen.69852

Abstract

In the present paper, we investigate the biological performance of the tricalcium phosphate ceramic (β-TCP) bone substitute combined with the fluorapatite (Fap). Porous biocomposites consisting of β-tricalcium phosphate (β-TCP) with 26.5% fluorapatite (Fap) were elaborated and characterized in order to evaluate its potential application in bone graft substitute. Bioactivity was determined with *in vivo* and *in vitro* tests by immersion of samples in simulated fluid body (SBF) for several periods of time. Clinical, radiological, and histological assessments were then carried out to evaluate the biological properties of developed β-TCP-26.5% Fap composites. An *in vivo* investigation revealed the biological properties of the prepared macroporous scaffolds, namely, biocompatibility, bioactivity, biodegradability, and osteoconductivity. The morphological characteristics, granule size, and chemical composition were indeed found to be favorable for osseous cell development. All histological observations of the preliminary *in vivo* study in the tibia of rabbits proved the biocompatibility and the resorption of the investigated bioceramic. In contrast, the implantation period will have to be optimized by further extensive animal experiments.

Keywords: bone substitute, tissue engineering, bioceramic, tricalcium phosphate, *in vivo*, *in vitro*, implant

1. Introduction

Tissue engineering applies methods from materials engineering and life sciences to create artificial constructs for regeneration of new tissue. Even though a range of tissues has been studied, the translation of engineered tissues to clinical applications has been limited [1]. Researchers in bone tissue engineering are working to develop alternatives to allogenic and

autologous bone grafts in order to address the growing needs of the population, and much of the research is scaffold based [2–7].

Calcium phosphate ceramics have been extensively used to produce porous scaffolds due to their bone-like chemical composition as well as excellent biological properties, including biocompatibility and osteoconductivity [8–11]. The use of these bioceramics was always restricted because of its fragility and the weak rupture resistance [12]. Hence, there was a need for maximizing mechanical properties of tricalcium phosphate β-TCP suitable for orthopedic applications. In recent investigation, a β-TCP-fluorapatite (Fap) composite has been developed for biomedical applications [13]. These β-TCP-Fap have shown a good combination of compressive strength (95 MPa), flexural strength (15 MPa), and fracture toughness (2.9 MPa $m^{1/2}$) [14]. Pure fluorapatite is known to possess a potential advantage with its high chemical stability and aptitude to delay caries' process without the biocompatibility degradation [15]. In addition, it has a much lower solubility in biological fluid than hydroxyapatite. In several studies, it has been proved that the amount of the released fluoride ions F^- affects directly cell attachment, proliferation, morphology, and differentiation of osteoblast cells [16, 17]. It is known that the fluorine ion itself enhances mineralization and crystallization [17]. Since such bioceramic β-TCP-26.5% wt% Fap composition has never been investigated *in vitro* and *in vivo* response as bone substitute. Among various properties, biological response of the developed composites should be evaluated in the light of its potential used in tissue engineering. It worth to note that all newly developed biomaterials are subjected to be approved based on their *in vivo* response results. In fact, *in vitro* experiments cannot produce significant evidences toward the biocompatibility of the investigated materials due to the absence of several hormones and enzymes [18].

In view of the above, the aim of this study is to investigate the bioactivity response of the new biphasic ceramic *in vitro* in simulated fluid body (SBF) and to evaluate its biocompatibility and also the process of bone regeneration in rabbits. The clinical, radiological, and histological assessments were performed.

2. Materials and methods

2.1. Materials

In order to elaborate β-TCP-Fap composites, the used materials are the commercial tricalcium phosphate (Fluka) and synthesized fluorapatite. The Fap powder was synthesized by the precipitation method [19]. In order to improve the biocompatibility of the fluorapatite and the strength of tricalcium phosphate effectively and to search for an approach to produce high performances of the tricalcium phosphate-fluorapatite ceramics. In this study, Fap has been used with a fixed 26.5 wt% amount because the human bone contains 1 wt% of fluorine approximately [20]. Estimated quantities of each powder were milled with absolute ethanol and treated by ultrasound machine for 20 min. The milled powder was dried in a low temperature oven at 80°C to eliminate the ethanol and generate a finely divided powder.

http://dx.doi.org/10.5772/intechopen.69852

The sintered samples used in *in vitro* study [21] were prepared using a molding process to form pellets of 10 mm ϕ × 2 mm of thickness (**Figure 2a**). The details of process optimization, density value, and microstructure could be found elsewhere [22]. All the samples used in the study had almost the same surface area and volume. It is worth noting that the experiments were repeated at least three times. At the end of experiments, all the samples were characterized by various technical tools. Scanning electron microscopy (SEM) was done to reveal the changes in topographical features and to visualize calcium phosphate crystals, the final products for the β-TCP-Fap reaction.

In order to obtain three-dimensional bioceramic for the *in vivo* evaluation, the β-TCP-26.5% Fap samples were prepared using polymeric sponge replication method [23–27]. This technique is based on the reproduction of a polymer foam with open cells by impregnation of a ceramic slurry and removing the support by thermal treatment (**Figure 1b**). This later was optimized based on thermal analysis [28]. Based on previous studies [13], the composite samples were sintered at 1300°C for 90 nm. Helium porosimetry and the Archimedes method were used for investigating density and porosity (both open and closed) of sintered samples.

The mechanical strength of the obtained macroporous biphasic ceramic β-TCP-26.5% Fap was also determined by Lloyd testing machine. The specimens used for compression test were prepared into cylinders (9.0 mm in diameter and 18.0 mm in length) as instructed in ASTM standards C1424-15.

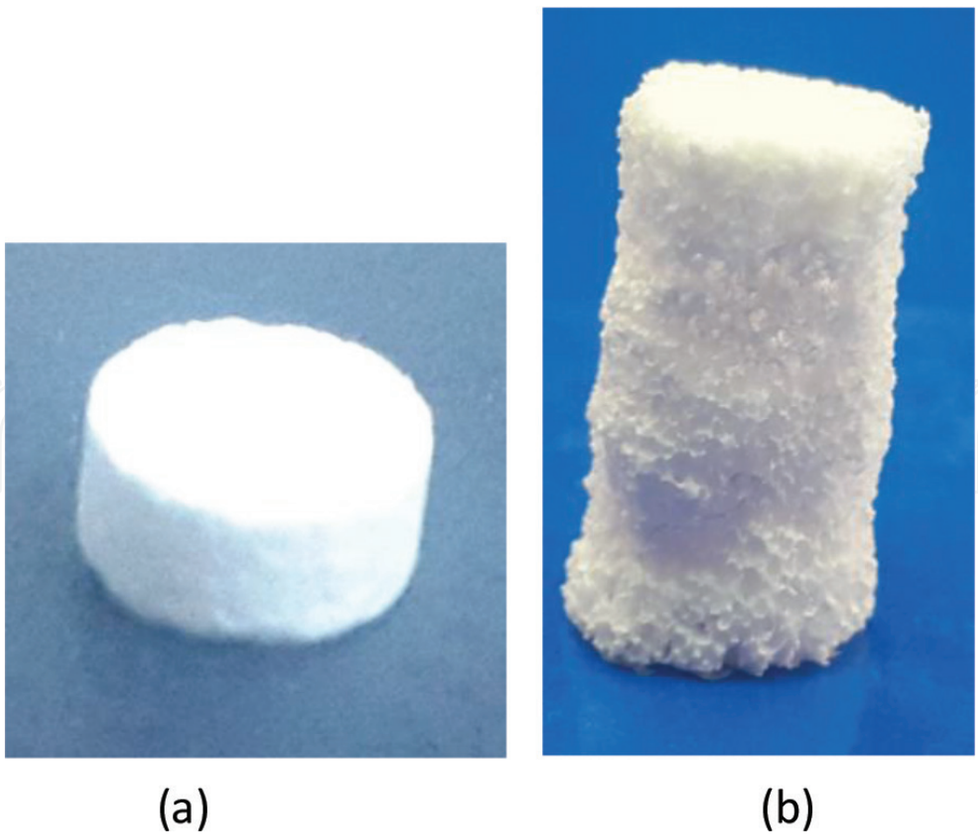

Figure 1. Photograph of the tested specimens: (a) for *in vitro* tests and (b) for *in vivo* tests.

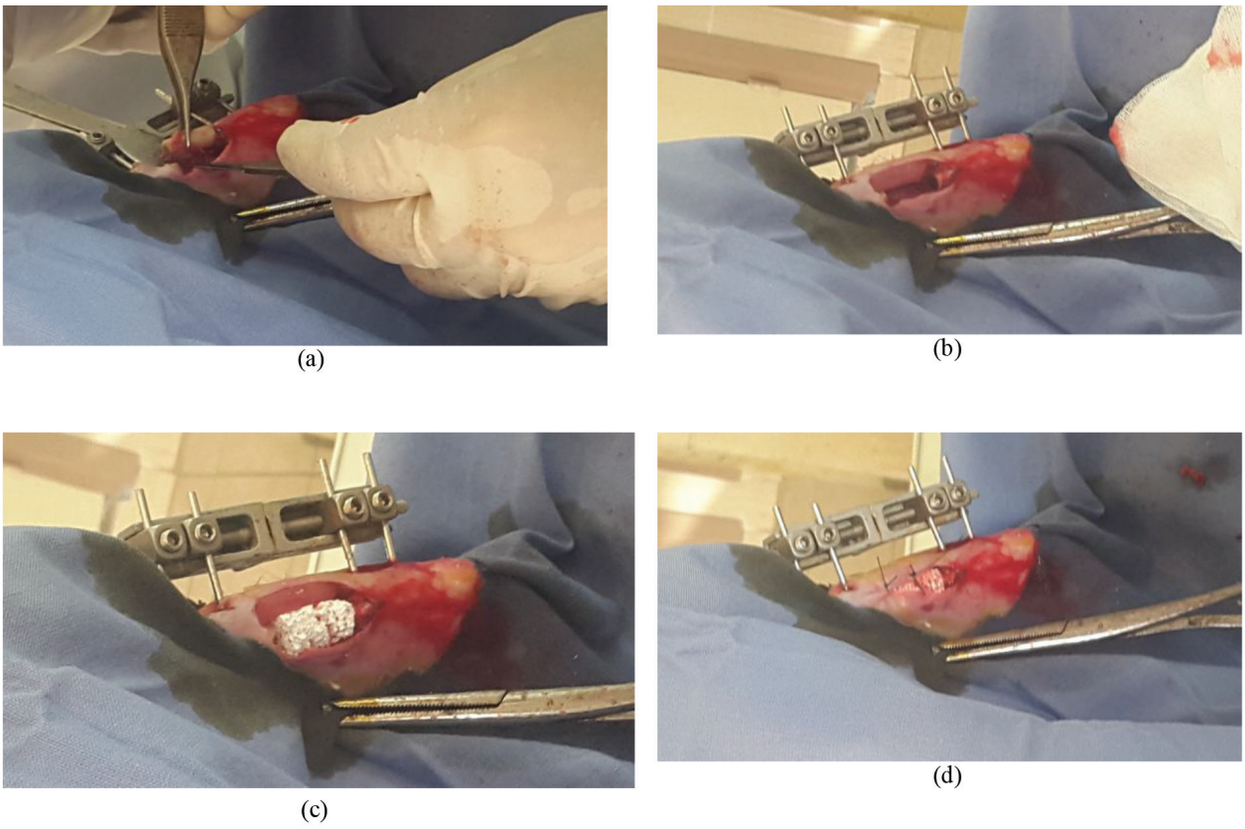

Figure 2. Digital camera images: (a and b) showing the implantation site and (c and d) β-TCP-26.5% Fap scaffold implanted inside the tibia of rabbit.

2.2. Scanning electron microscopy

The microstructure of the sintered samples was observed by scanning electronic microscopy (SEM) (JSM-5400). The observations were performed on gold-coated specimens and investigated at an acceleration voltage of 15 kV for all samples.

2.3. *In vitro* bioactivity assessment in SBF

Bioactivity was checked through tests of immersion in simulated body fluid (SBF) [21]. In order to study the dissolution behavior of the β-TCP-Fap in physiological environment, the *in vitro* dissolution study was carried out by immersing batches of samples for six different time periods of 4, 24, and 49 h and 6, 12, and 30 days. The initial pH of the solution was kept at 7.42 with tris(hydroxymethyl)-aminomethane and hydrochloric acid. The solution temperature was maintained at body temperature, i.e., 37°C using an incubator. 100 ml of SBF solution was used for each sample. The ion concentration of the SBF is shown in **Table 1**.

2.4. *In vivo* implantation experiments

2.4.1. Surgical procedures

Given the closeness of the metabolism of rabbit s to humans, we estimated that the resorption kinetics in rabbits can fairly be assumed to be similar to that in humans.

Ion	Concentration (mmol/l)	
	SBF	**Human plasma**
Na^+	142.0	142.0
K^+	5.0	5.0
Mg^{2+}	1.5	1.5
Ca^{2+}	2.5	2.5
Cl^-	103.0	147.8
HCO^{3-}	27.0	4.2
HPO_4^{2-}	1.0	1.0
SO_4^{2-}	0.5	0.5
pH	7.2–7.4	7.4

Table 1. Ion concentrations of the human blood plasma and the SBF solution.

In this experiment, two New Zealand white rabbits with an average weight of 2.1 kg were used. The β-TCP-26.5% Fap pellets were sterilized by irradiation from a ^{60}Co gamma irradiation source at a dose of 25 Gy (Equinox, UK) using standard procedures for medical devices. The surgical procedure earned approval from ethical committee of the Tunisian Association of Laboratory Animal Sciences according to the ICLAS ethical guidelines for researchers to committee. All animals were subject to general, backed with local, anesthesia through intramuscular administration of 10 mg/kg ketamine hydrochloride (Ketaminol®, Germany) and 0.1 mg/kg xylazine (Rompun®, France).

In each animal, one lower limb was prepared aseptically for surgery. After shaving the lower limb segment and disinfecting it with Betadine®, a 4 cm skin incision was made medially over the leg, and the tibia was exposed subperiosteally. A 10 mm bony segmental defect was then created by two osteotomies in the middle portion of the tibia. The osteotomy was performed with an oscillating saw at a right angle to the axis of the bone. The defect was then filled with a suitably shaped bioceramic (**Figure 2**(**a**–**d**)). To stabilize the tibia and maintain a direct contact between bioceramic and the bone, a mini-stainless steel monoplanar fixator was used. Four pins were inserted through the skin into the bone and then attached to a steel rod outside the limb. Next, the wound was closed for the periosteum and the subcutaneous tissues using a resorbable suture. Finally, a postoperative bandage was made with a sterile compress after local application of Betadine gel®. After the surgical procedure, all the animals were given postoperative care.

Radiographic images were taken at 4 days, 6 weeks, and 12 weeks after implantation to assess the stability of the bioceramic and follow the general structural health of the operated bone; anteroposterior and lateral radiographs of each operated leg were made. Radiographs were obtained using an X-ray machine.

2.4.2. Histological evaluation

For microscopic evaluation and to evaluate composite biocompatibility and the biological response of the bone tissue in contact, histological studies were conducted after 12 postoperative

weeks. The animals were euthanized, and then the sites of implantations were grossly examined for any evidence of tissue reaction, and tibia bones with the test implant materials were removed and fixed in 10% formaldehyde during 24 h to immobilize the cells for subsequent histological studies. The timing was selected to assess the performance of the biomaterial bone formation before degradation. The samples were then dehydrated in three successive acetone baths. Next, they were placed in methyl methacrylate (MMA) with decalcification. Sections of 4 μm thick were debited along a transverse plane using a sliding microtome (Reichert-Jung). Once colored with hematoxylin eosin, the cut was mounted between slide and slip cover. The colored cuts were observed through a binocular microscope (Olympus® CX-21i), and the observations were photographed with various magnifications using the digital camera.

3. Results and discussion

3.1. Bioactive surface characterization (*in vitro* test): SEM results

To investigate the dissolution behavior of the samples, SEM was performed. It has been seen (**Figure 3b**) that the surface of soaked sample becomes more porous after 4 h immersion, which is a signature that dissolution has occurred. The dissolution affects the strength by

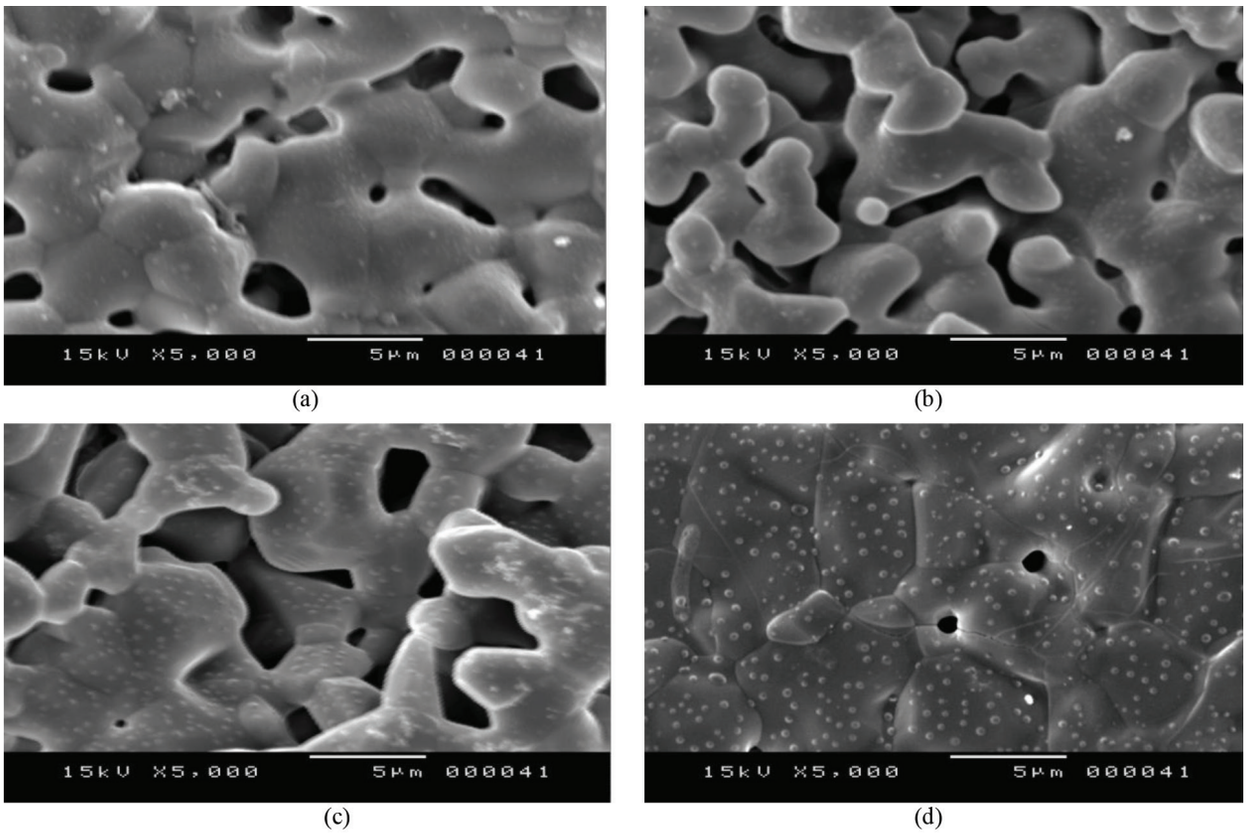

Figure 3. SEM micrographs: (a) sintered β-TCP-26.5% Fap before immersion in SBF, (b) development of porous regions after 4 h of dissolution process, (c) nucleation of apatite crystals after 24 h, and (d) pores filled with formed apatite after 48 h.

increasing the porosity and weakening the grain boundary. After 24 h immersion, the microstructural observation indicates that the surfaces of grains appear mottled.

SEM (**Figure 3c**) indicates precipitation of nodular apatite on the biocomposite grains. With the increase in immersion time, the quantity and size of these apatite particles increase gradually. We note the formation of apatite agglomerate. The apatite formation fills the pores and increases the density and strength of the material (**Figure 3d**). Moreover, EDS analysis also performed on the surface of the soaked sample revealed the presence of calcium and phosphorous elements on the surface, with Ca-P equal to 1.67. This Ca-P ratio is in accordance to stoichiometric biological apatite and indicated that the deposit form during SBF conditioning is apatite layer.

SEM images depict the change in the topographical features recorded for various time intervals during experiment. In fact, the precipitation is more prevalent after immersion showing the formation of bone-like apatite layer due to the dissolution of Ca^{2+} and PO_4^{3-}, followed by deposition of Ca-P (**Figure 4a**). Higher magnification SEM micrograph reveals that particles of apatite grow in a flake-like form and many of these formed agglomerates on the surface of sample (**Figure 4c**). After soaking for 12 days, in the surface of sample, tiny ball apatite particles that formed porous agglomerates were found (**Figure 5b and c**). This outcome has been found by previous studies that proved that the apatite formation occurs in two stages: a formation of globular particles followed by appearance of aggregate which joined together to form a covering layer [29].

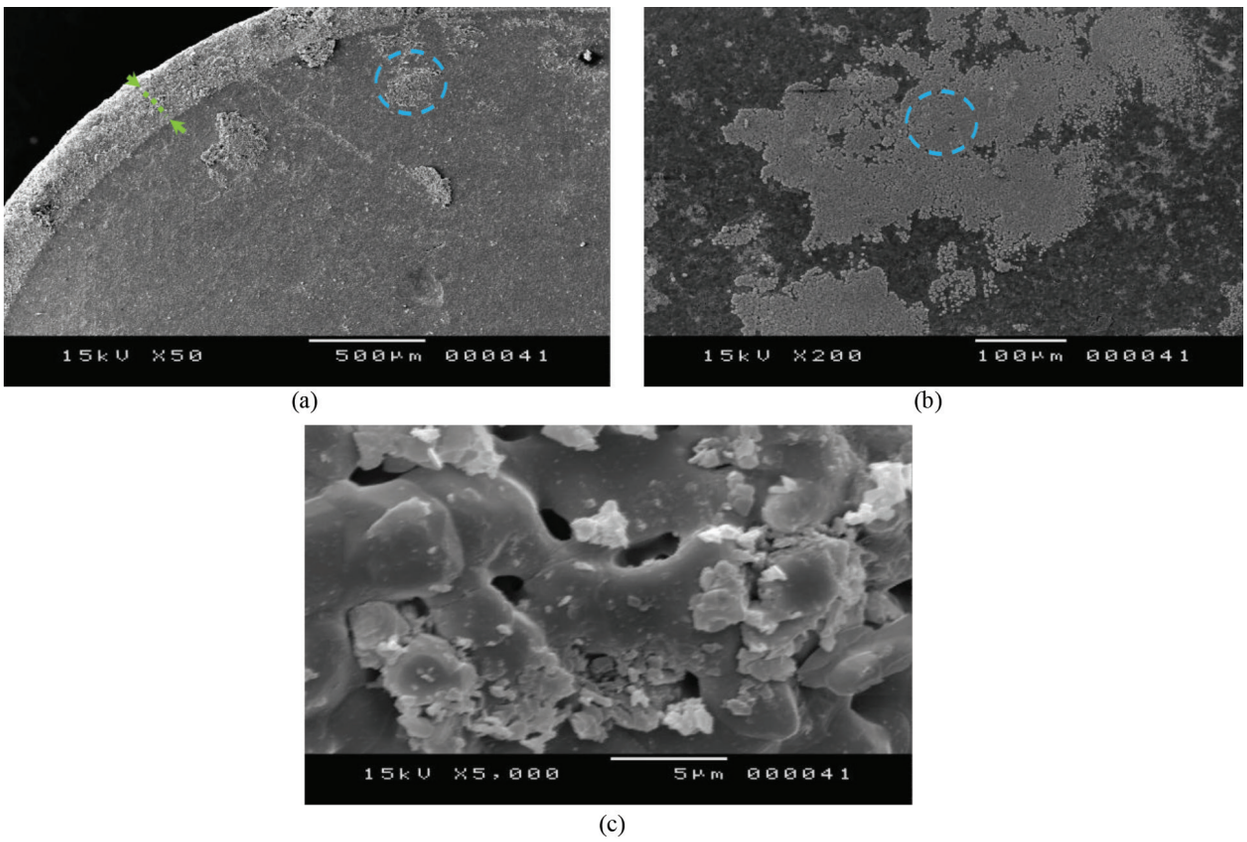

Figure 4. SEM images show the topographic features of β-TCP-26.5% Fap sample after 6 days of dissolution period, (b) is a magnified image of a selected zone from (a), and (c) apatite grows in a flake-like form.

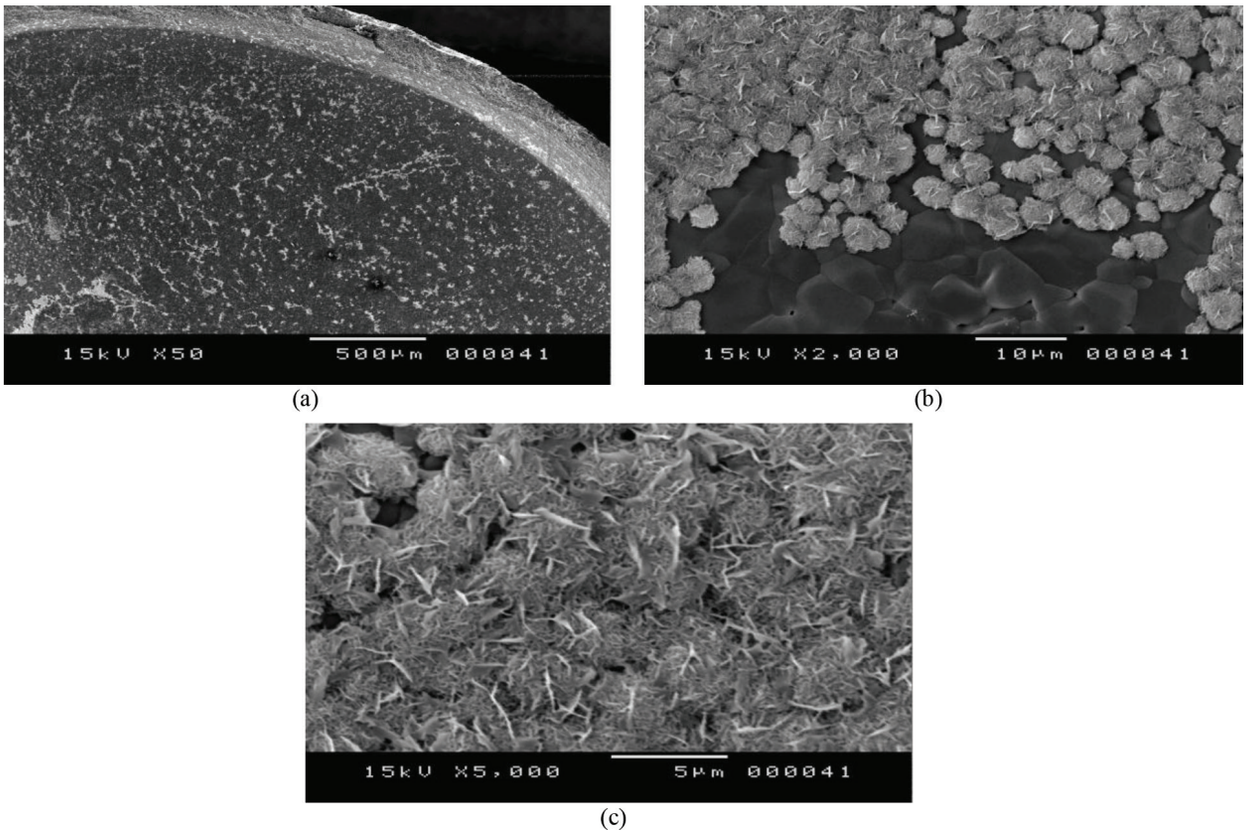

Figure 5. SEM micrographs of sample surface after 12 days of immersion (a) showed the deposit apatite layer, (b) porous agglomerates of apatite particles, and (c) needle-like apatite crystals.

After 30 days of immersion in SBF, a thick and dense mineral layer was formed on the specimen surface, and mineral crystals covered almost the surface of the specimen. **Figure 6b** reveals higher magnification micrograph of the region marked in **Figure 6a** showing typical entanglement of the reprecipitated leaf-like or plate-like crystals (**Figure 6c**).

It is well known that the dissolution of the initial Ca-P compounds has occurred until the oversaturation of the solution, thus inducing the reprecipitation of crystals [10, 30]. The bioactivity of calcium phosphate and other materials has been related to their propensity to nucleate apatite crystals [31]. The presence of bone-like apatite agglomerate on the surface of any implant is always considered as a positive biological response. Therefore, the findings that β-TCP-26.5% Fap shows extensive precipitation of apatite are a clear indication of bioactivity.

3.2 Preliminary *in vivo* evaluation

3.2.1. Microstructure and mechanical characterization of bioceramic scaffolds

The SEM analysis for β-TCP-26.5% Fap scaffolds presented highly porous and interconnective pore architecture with porosity of 75% which has an open porosity 71%. As can be observed in **Figure 7**, the ceramic foams appeared to be macroporous with different pore sizes. The pore size distribution seemed to be uniform. Pore sizes were roughly about 300 μm, which is above the critical value of 100 μm to allow bone [32].

http://dx.doi.org/10.5772/intechopen.69852

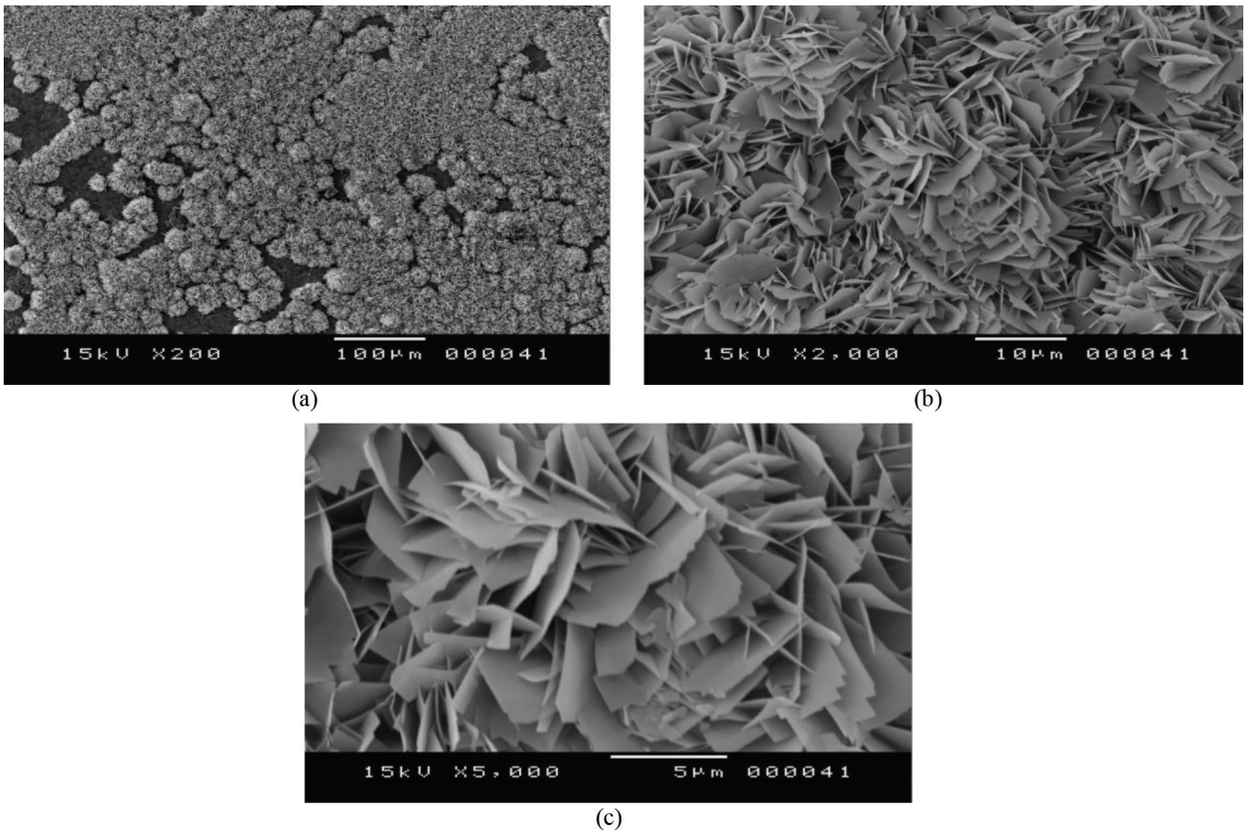

Figure 6. SEM images of β-TCP-26.5% Fap sample after soaking in SBF for 30 days: (a) joined aggregate forms a covering layer, (b) showing needle-like and plate-like crystals, and (c) is a magnified image of selected zone from (b).

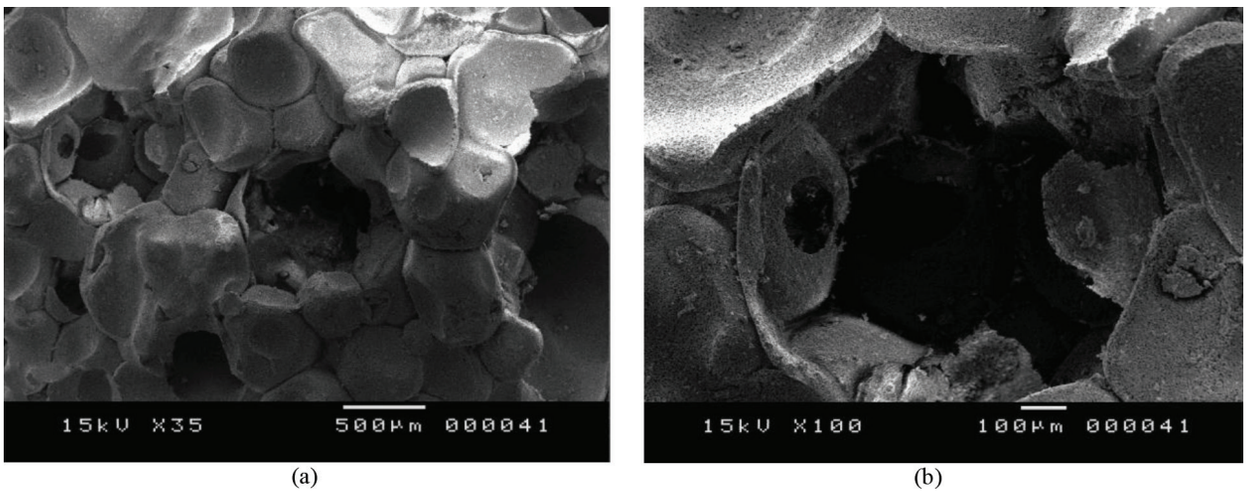

Figure 7. (a) SEM images of porous β-TCP-26.5% Fap and (b) zoom.

The mechanical strength of the β-TCP-26.5% sintered foam was plotted as function of porosity (**Figure 8**). At least six samples were tested under compression test condition. Average strength values were calculated. The maximum error obtained was found to be less than 5%. As expected, the compressive strength decreased with increasing porosity. Moreover, the compressive strength presented a sharp decrease as soon as macropores are introduced.

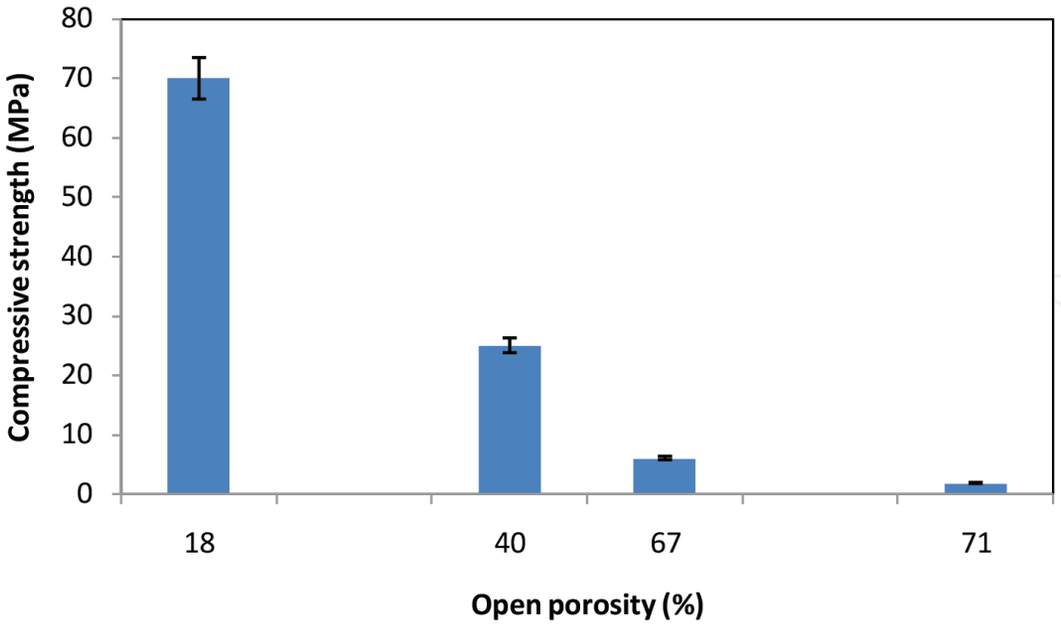

Figure 8. Compressive strength versus open porosity of β-TCP-26.5% bioceramics.

3.2.2 Clinical control and radiological findings

During the postoperative, the daily clinical evaluation exhibited no sign of surgical site infection (i.e., swelling, redness, or wound disunion) on the operated rabbits, which had overcome the tibia osteotomy. After 6 weeks postimplantation, the radiographs showed healing of the host bone and mild degeneration of the implanted bioceramic. The bioresorption is partly revealed by the change in implant dimension (**Figure 9b**).

At 12 postoperative weeks, the radiograph showed complete healing of the host bone and disappearance of the implanted biomaterial (**Figure 9c**). In fact, bone consolidation was noted in the two rabbits.

3.2.3. Organ harvesting and general observations

After completion of the expected implantation time (12 postoperative weeks), the operated rabbits were sacrificed, and the samples were extracted immediately and then stored in an ethanol or BBS solution prior to the histological study. The explants were then transferred to the laboratory of histology and embryology for inclusion in resin and histological study. Given the small amount of data currently being processed, we cannot conclude on the osteoconductive potential of our implant. However, it should be noted that no major problems occurred during the operation or during the implementation periods. In addition, observation of the explants also showed almost complete dissolution of the elaborated implant and the formation of a new neoformed bone (**Figure 10**). This observation will be confirmed by the histological study.

3.2.4. Histological analysis

Although tricalcium phosphate and fluorapatite are reported to be biocompatible *in vivo*, the combination of these phases is not yet tested *in vivo*. Therefore, the biocompatibility

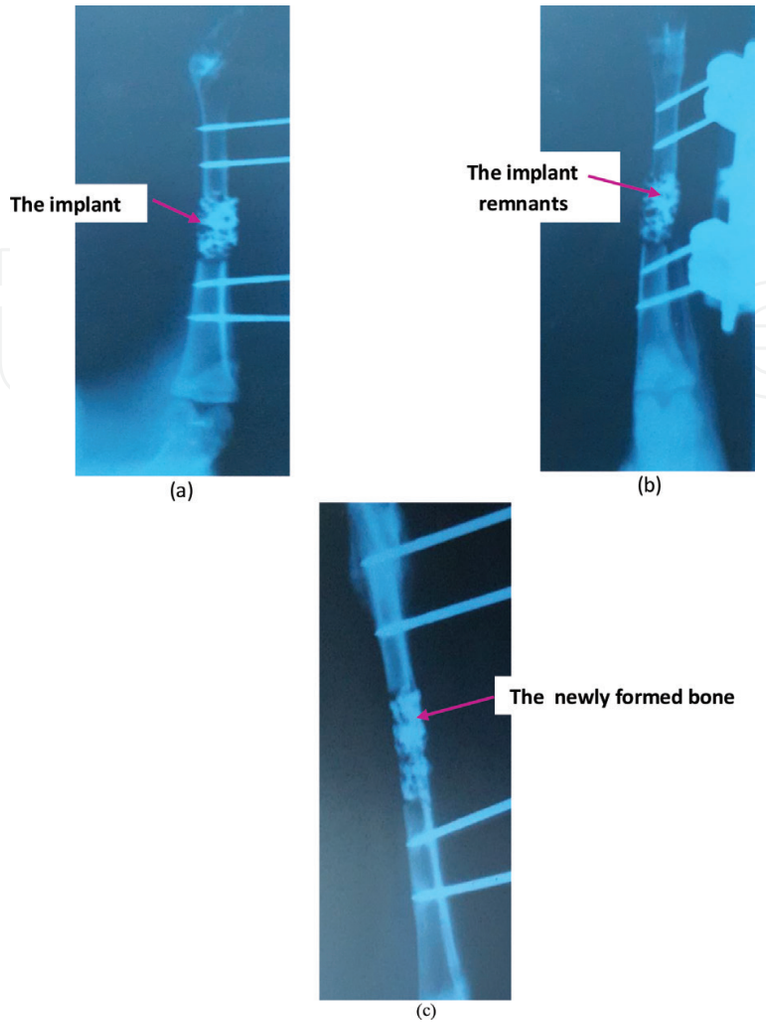

Figure 9. X-ray radiographs of postimplant rabbit's tibia: (a) after 4 days, (b) after 6 postoperative weeks, and (c) after 12 postoperative weeks.

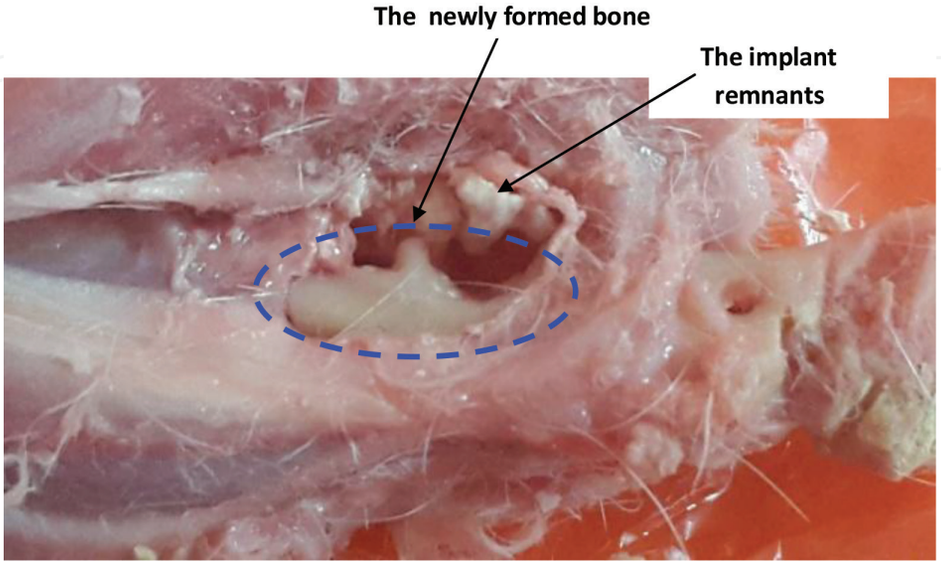

Figure 10. Extraction of the implant after 12 postoperative weeks.

evaluation of this biphasic material would be of great interest. It is to be noted here that in the investigated composite, the major phase is β-TCP, which is well known for its bioresorbability. However, in our case, the resorption is limited due to the presence of second-phase fluorapatite.

Figure 11 illustrates the representative optical microscopy images of the histological sections of bone implant interface. A cellular infiltrate, predominantly composed of macrophages, was observed. Although the short-term implantation of 12 weeks is being carried out in this investigation, the experimental observations should provide clear indication about the biocompatibility *in vivo*. These findings revealed that β-TCP-26.5% Fap is biocompatible and appears to induce acceptable *in vivo* response. However, it appeared that the resorption rate of this bioceramic was far too low to induce neobone formation after 12 weeks postimplantation. Despite these results, the proposed material presented markedly better mechanical properties than monophasic β-TCP [14]. Hence, the incorporated fluorapatite can be used to modulate the biological and the mechanical properties. Thus, the challenge is to find a balance between the biological performance and the changes in mechanical behavior provoked by both the macroporosity and the composite effects. Further encouragement from these results is that the novel bioceramic should have an attracted potential as bioactive coating for orthopedic. Such application required long-term and sufficient mechanical stability when under physiological stresses associated with locomotion to not detach from the implant surface [33].

Considering the importance of the time required for integration and osteointegration, which is determined by the newly formed bone at the host bone-material interface, we should investigate the biological response according to ISO-10993 guidelines. Additionally, the implantation period will have to be optimized by further extensive animal experiments. An *in vitro cell* culture model can be also an *alternative* to study the cytocompatibility of the novel bioceramic as well as other research [34–36].

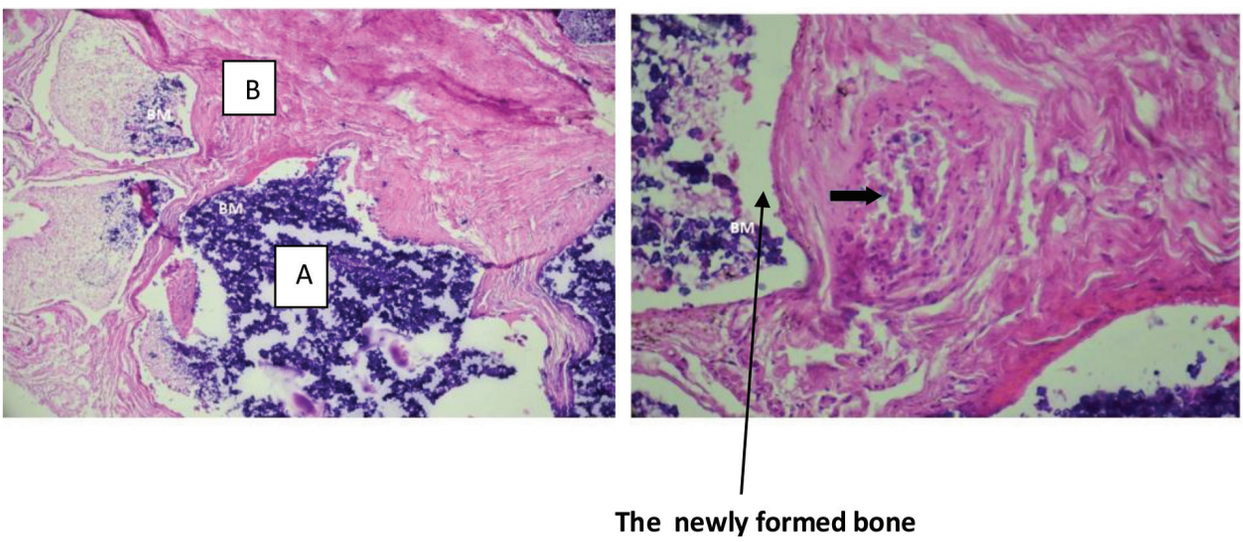

Figure 11. Histological sections of β-TCP-26.5% Fap scaffold after 12 weeks of implantation in rabbit. (A) Fibrous tissue surrounding the biomaterial. (B) Inflammatory infiltrates around degradated biomaterial (➡).

http://dx.doi.org/10.5772/intechopen.69852

4. Conclusion

In this study, a novel biphasic material that consisted of two major phases of tricalcium phosphate and fluorapatite was investigated. During bioactivity experiments, the bone substitute material exhibited to be able to produce porous apatite layer *in vitro*. The combination of dissolution and precipitation is found to be the mechanism of apatite formation. The results showed that fluoride released ion decreased the dissolution rate by improving the crystallization.

A preliminary *in vivo* investigation revealed that the new bioceramic scaffold with highly porous architecture exhibits biocompatibility. It can be concluded that β-TCP-26.5% Fap may take few more weeks for deposition of neobone. Besides, there are many aspects related to *in vivo* behavior that need further *in vivo* results in order to confirm or improve the formulation of the porous bioceramic that should promote both osteoconductive and resorption processes.

Author details

Achouak Elghazel[1]*, Rym Taktak[2], Jamel Bouaziz[1], Slim Charfi[3] and Hassib Keskes[4]

*Address all correspondence to: elgazelachwak@live.fr

1 Laboratory of Industrial Chemistry, National School of Engineers of Sfax, Sfax, Tunisia

2 Materials Engineering and Environment Laboratory, National School of Engineers of Sfax, Sfax, Tunisia

3 Department of Pathology CHU Habib Bourguiba, Sfax, Tunisia

4 Orthopedics-Traumatology Research Unit, Faculty of Medicine of Sfax, Tunisia

References

[1] Lanza R. Principles of Tissue Engineering, 4th ed. USA: Elsevier; 2014

[2] Gómez S, Vlad MD, López J, Fernández E. Design and properties of 3D scaffolds for bone tissue engineering. Acta Biomaterialia. 2016;**42**:341-350

[3] Reno CO, Lima BFAS, Sousa E, Bertran CA. Scaffolds of calcium phosphate cement containing chitosan and gelatin. Materials Research. 2013;**16**:1362-1365

[4] Hea D, Zhuanga C, Xub S, Kec X, Yanga X, Zhangc L, Yangc G, Chend X, Moud X, Liue A, Goua Z. 3D printing of Mg-substituted wollastonite reinforcing diopside porous bioceramics with enhanced mechanical and biological performances. Bioactive Materials. 2016;**1**:85-92

[5] Stevens MM. Biomaterials for bones tissue engineering. Materials Today. 2008;**11**:18-25

[6] Bohner M, Galea L, Doebelin N. Calcium phosphate bone graft substitutes: Failures and hopes. Journal of the European Ceramic Society. 2012;**32**(Special Issue: E Cer S XII, 12th Conference of the European Ceramic Society):2663-2671

[7] Yea X , Caia S, Xub G, Doua Y, Hub H, Yeb X. Preparation and in vitro evaluation of mesoporous hydroxyapatite coated β-TCP porous scaffolds. Materials Science and Engineering. 2013;**33**:5001-5007

[8] Szubert M, Adamska K, Szybowicz M, Jesionowski T, Buchwald T, Voelkel A. The increase of apatite layer formation by the poly(3-hydroxybutyrate) surface modification of hydroxyapatite and β-tricalcium phosphate. Materials Science and Engineering. 2014;**34**:236-244

[9] Azevedo AS, Sá MJC, Fook MVL, Nóbrega Neto PI, Sousa OB, Azevedo SS, Teixeira MW, Costa FS, Araújo AL. Use of chitosan and β-tricalcium phosphate, alone and in combination, for bone healing in rabbits. Journal of Materials Science Materials in Medicine. 2014;**25**:481-486

[10] Zhang Y, Li S, Wu C. The in vitro and in vivo cementogenesis of CaMgSiO bioceramic scaffolds. Journal of Biomedical Materials Research. Part A. 2014;**102**:105-116

[11] Levent Aktuğa S, Durdu S, Yalçınc E, Çavuşoğluc K, Usta M. Bioactivity and biocompatibility of hydroxyapatite-based bioceramic coatings on zirconium by plasma electrolytic oxidation. Materials Science and Engineering. 2017;**71**:1020-1027

[12] Boslama N, Chevalier Y, Bouaziz J, Ben Ayed F. Influence of the sintering temperature on Young's modulus and the shear modulus of tricalcium phosphate—Fluorapatite composites evaluated by ultrasound techniques. Materials Chemistry and Physics. 2013;**141**:289-297

[13] Elghazel A, Taktak R, Bouaziz J. Determination of elastic modulus, tensile strength and fracture toughness of bioceramics using the flattened Brazilian disc specimen: Analytical and numerical results. Ceramics International. 2015;**41**:12340-12348

[14] Elghazel A, Taktak R, Bouaziz J. Combined numerical and experimental mechanical characterization of a calcium phosphate ceramic using modified Brazilian disc and SCB specimen. Materials Science and Engineering A. 2016;**670**:240-251

[15] Ben Ayed F, Bouaziz J. Sintering of tricalcium phosphate–fluorapatite composites by addition of alumina. Ceramics International. 2008;**34**:1885-1892

[16] Tredwin CJ, Young AM, Abou Neel EA, Georgiou G, Knowles JC. Hydroxyapatite fluorhydroxyapatite and fluorapatite produced via the sol-gel method: dissolution behaviour and biological properties after crystallization. Journal of Materials Science Materials in Medicine. 2014;**25**:47-53

[17] Nathanaela J, Mangalarajc D, Hongb SI, Masudad Y, Rheee YH, Kime HW. Influence of fluorine substitution on the morphology and structure of hydroxyapatite nanocrystals prepared by hydrothermal method. Materials Chemistry and Physics. 2013;**137**:967-976

[18] Nath S, Basu B, Mohanty M, Mohanan PV. In vivo response of novel calcium phosphate-mullite composites: results up to 12 weeks of implantation. Journal of Biomedical Materials Research Part B: Applied Biomaterials. 2009;**90**:547-557

[19] Ben Ayed F, Bouaziz J, Bouzouita K. Pressureless sintering of fluorapatite under oxygen atmosphere. Journal of the European Ceramic Society. 2000;**20**:1069-1076

[20] Moreno EC, Kresak M, Zahradink RT. Nature. 1974;**247**:64-65

[21] Kokubo T, Kushitani H, Sakka S, Kitsugi T, Yamamwo T. Solutions able to reproduce in vivo surface structure changes in bioactive glass-ceramic A-W. Journal of Biomedical Materials Research 1989;**24**:721-734

[22] Bouslama N, Ben Ayed F, Bouaziz J. Effect of fluorapatite additive on densification and mechanical properties of tricalcium phosphate. Journal of the Mechanical Behavior of B iomedical Materials 2010;**3**:2-13

[23] Lee JH, Kim HE, Kohr YH. Highly porous titanium (Ti) scaffolds with bioactive microporous hydroxyapatite/TiO_2 hybrid coating layer. Materials Letters. 2009;**63**:1995-1998

[24] Li J, Li S, Van Blitterswijk C, De Groot K. A novel porous Ti6Al4V: Characterization and cell attachment. Journal of Biomedical Materials Research. Part A. 2005;**73**:223-233

[25] Lee JH, Kim HE, Shin KH, Koh YH. Improving the strength and biocompatibility of porous titanium scaffolds by creating elongated pores coated with a bioactive, nanoporous TiO_2 layer. Materials Letters. 2010;**64**:2526-2529

[26] Hsu HC, Hsu SK, Wu SC, Wang PH, Ho WF. Design and characterization of highly porous titanium foams with bioactive surface sintering in air. Journal of Alloys and Compounds. 2013;**575**:326-332

[27] Wang C, Chen H, Zhu X, Xiao Z, Zhang K, Zhang X. An improved polymeric sponge replication method for biomedical porous titanium scaffolds. Materials Science and Eng ineering C. 2017;**70**:1192-1199

[28] Chaari K, Ben Ayed F, Bouaziz J, Bouzouita K. Elaboration and characterization of fluorapatite ceramic with controlled porosity. Materials Chemistry and Physics. 2009;**113**:219-226

[29] Martíneza M, Meseguer-Olmob L, Bernabeu Esclapezb A, Velásqueza PA, De Aza PN. In vitro behavior of α-tricalcium phosphate doped with dicalcium silicate in the system Ca_2SiO_4–$Ca_3(PO_4)_2$ I. Materials Characterization. 2012;**63**:47-55

[30] Hua H, Liua X, Dinga C. Preparation and in vitro evaluation of nanostructured TiO_2/TCP composite coating by plasma electrolytic oxidation. Journal of Alloys and Compounds. 2010;**498**:172-178

[31] Priya A, Nath S, Biswas K, Basu B. In vitro dissolution of calcium phosphate-mullite composite in simulated body fluid. Journal of Materials Science Materials in Medicine. 2010;**21**:1817-1828

[32] Hench LL. Bioceramics. Journal of the American Ceramic Society. 1998;**81**:1705-1728

[33] Zhang BG, Myers DE, Wallace GG, Brandt M, Choong PF. Bioactive coatings for orthopaedic implants-recent trends in development of implant coatings. International Journal of Molecular Sciences. 2014;**15**:11878-11921

[34] Liu H, Li H, Cheng W, Yang Y, Zhu M, Zhou C. Novel injectable calcium phosphate/chitosan composites for bone substitute materials. Acta Biomaterialia. 2006;**2**:557-565

[35] Ulum MF, Arafat A, Noviana D, Yusopa AH, Nasutiona AK, Abdul Kadir MR, Hermawan H. In vitro and in vivo degradation evaluation of novel iron-bioceramic composites for bone implant applications. Materials Science and Engineering C. 2014;**36**:336-344

[36] Liu W, Zhai D, Huan Z, Wu C, Chang J. Novel tricalcium silicate/magnesium phosphate composite bone cement having high compressive strength, in vitro bioactivity and cytocompatibility. Acta Biomaterialia. 2015;**21**:217-227